

Stress Generation by Solvent Absorption and Wrinkling of a Cross-Linked Coating atop a Viscous or Elastic Base

Soumendra K. Basu,* Alon. V. McCormick, and L. E. Scriven

Coating Process Fundamentals Program, Department of Chemical Engineering & Materials Science, University of Minnesota, 421 Washington Avenue SE, Minneapolis, Minnesota, 55455

Received February 28, 2006. In Final Form: April 20, 2006

An in-plane constrained cross-linked gel layer absorbs an equilibrium amount of solvent and experiences in-plane compressive stress. A stability analysis of such an elastic gel layer that is attached to either a viscous or an elastic bottom layer atop a rigid substrate is considered. The effects of the top and bottom layer moduli (E_t and E_b), the bottom-to-top layer thickness ratio (H/h), and the polymer solvent interaction parameter (χ) on the critical condition of wrinkling, wrinkle wavelength, and amplitude are examined. When the bottom layer is viscous, the compressed top layer is always unstable, and wrinkling is rate-controlled. The viscous flow of the bottom layer governs the rate and determines the fastest growing wavelength. As E_t rises, the bending stiffness of the elastic layer does as well, and so the fastest growing wavelength (λ_m) rises and the equilibrium amplitude (A_e) falls. As H/h rises, the constraint of the rigid substrate diminishes, and so λ_m and A_e rise. As χ falls or as the solvent has higher affinity for the polymeric gel, λ_m falls and A_e rises because better solvents create higher compressive strain that promote low-wavelength, high-amplitude wrinkles. When the bottom layer is elastic, a critical compressive stress exists. If the generated compressive stress by solvent absorption is greater than the critical stress, the top layer wrinkles. It was found that wrinkling is most likely at intermediate E_t , low E_b , high H/h , and low χ . Further, lower χ , higher H/h , and lower E_b were found to promote higher equilibrium amplitude and higher wavelength wrinkles.

1. Introduction

A solidified polymeric coating with two layers atop a rigid substrate can wrinkle if the top layer is put into high enough in-plane compressive stress. Under high enough in-plane compressive stress, the planar shape of the top layer becomes unstable with respect to buckling, and it deforms out of plane to produce wrinkles. The bottom layer can be either viscous^{1–3} or elastic^{4–6} at the time of wrinkle formation. Therefore, as a two-layer polymeric coating solidifies, predicting the in-plane stress generated in the top layer is critical for predicting whether the top layer would wrinkle.

Many authors have analyzed stress generation in different layers of a multilayer system subjected to isotropic^{7,8} and anisotropic⁹ in-plane forces. During drying, curing, and subsequent processing, different layers in a multilayer coating can generate either in-plane tensile or compressive stress. Wrinkling under tension is explained by the so-called “tension field theory”.¹⁰ This paper examines the wrinkling of two-layer coatings atop a rigid substrate under compression by buckling instability.¹⁷ Generally, a multilayer coating under compression can buckle by two distinct processes. First, one or more layers can buckle out of plane and delaminate from the adjacent layer(s) to produce

blisters.^{18–23} Second, one or more layers can buckle without loosening the adhesion to the adjacent layer(s). The adjacent layer(s) deform(s) to accommodate the out-of-plane deformations of the buckled layer(s).^{24–28} All the examples of solidifying polymeric coatings examined^{6,29} were found to wrinkle by the second process, wherein the top layer buckled and the bottom layer conformed to the buckled shape.

The top layer can be put into compression by at least two distinct processes: first, by changing the temperature of the coating, provided that the different layers have different thermal expansivities and, second, by absorbing solvents in the top layer. Compressive stress generation and wrinkling by changing the

(10) “Tension field theory” accounts for wrinkling in thin free-standing layers under in-plane tension by assuming negligible flexural stiffness of the layer. The theory argues that, for such a layer, if the state of stress in the plane of the layer is such that one of the principal stresses is tensile and the other is zero or slightly compressive, the layer would wrinkle with wrinkles oriented in the direction of the tensile principal stress.^{11–15} A scaling analysis of the wavelength and amplitude of wrinkles produced under in-plane tension that complement the tension field theory is presented by Cerda et al.¹⁶

* Corresponding author. E-mail: soumendra.basu@gm.com. Tel: 91-9880518260.

- (1) Gorand, Y.; Doumenc, F.; Guerrier, B.; Allain, C. *Rheologie* **2003**, *3*, 22.
- (2) Basu, S. K.; Scriven, L. E.; Francis, L. F.; McCormick, A. V. *Prog. Org. Coat.* **2005**, *53*, 1.
- (3) Basu, S. K.; Scriven, L. E.; Francis, L. F.; McCormick, A. V.; Reichert, V. R. *J. Appl. Polym. Sci.* **2005**, *98*, 116.
- (4) Bowden, N.; Brittain, S.; Evans, A. G.; Hutchinson, J. W.; Whitesides, G. M. *Nature* **1998**, *393*, 146.
- (5) Bowden, N.; Huck, W. T. S.; Paul, K. E.; Whitesides, G. M. *Appl. Phys. Lett.* **1999**, *75*, 2557.
- (6) Basu, S. K.; Bergstreser, A. M.; Francis, L. F.; Scriven, L. E.; McCormick, A. V. *J. Appl. Phys.* **2005**, *98*, 063507.
- (7) Roll, K. J. *J. Appl. Phys.* **1976**, *47*, 3224.
- (8) Townsend, P. H.; Barnett, D. M.; Brunner, T. A. *J. Appl. Phys.* **1987**, *62*, 4438.
- (9) Finot, M.; Suresh, S. *J. Mech. Phys. Solids* **1996**, *44*, 683.

- (11) Reissner, E. *Proc. 5th Int. Congr. Appl. Mech.* **1939**, 88.
- (12) Mansfield, E. H. *Proc. R. Soc. London, Ser. A* **1977**, *316*, 475.
- (13) Miller, R. K.; Hedgepeth, J. M.; Weingarten, V. I.; Das, P.; Kahyai, S. *Comput. Struct.* **1985**, *20*, 631.
- (14) Pipkin, A. C. *Arch. Ration. Mech. Anal.* **1986**, *95*, 93.
- (15) Wu, C. H.; Canfield, T. R. *Q. Appl. Math.* **1981**, 179.
- (16) Cerda, E.; Mahadevan, L. *Phys. Rev. Lett.* **2003**, *90*, 074302.
- (17) Singer, S. J. *Phys. Rev. E* **2000**, *62*, 3736.
- (18) Crosby, K. M.; Bradley, R. M. *Phys. Rev. E* **1999**, *59*, R2542.
- (19) Audoly, B. *Phys. Rev. Lett.* **1999**, *83*, 4124.
- (20) Hutchinson, J. W.; He, M. Y.; Evans, A. G. *J. Mech. Phys. Solids* **2000**, *48*, 709.
- (21) Hutchinson, J. W.; Suo, Z. *Adv. Appl. Mech.* **1991**, *29*, 63.
- (22) Suo, Z. *J. Mech. Phys. Solids* **1995**, *43*, 829.
- (23) Pandey, R. K.; Sun, C. T. *Compos. Sci. Technol.* **1999**, *59*, 405.
- (24) Allen, H. G. *Analysis and Design of Structural Sandwich Panels*; Pergamon: London, 1969; p 156.
- (25) Biot, M. A. *Mechanics of Incremental Deformations*; John Wiley: New York, 1965.
- (26) Frostig, Y. *Int. J. Solids Struct.* **1998**, *35*, 183.
- (27) Hunt, G. W.; DaSilva, L. S.; Manzocchi, G. M. E. *Proc. R. Soc. London, Ser. A* **1988**, *417*, 155.
- (28) Niu, K.; Talreja, R. J. *Eng. Mech.* **1999**, *125*, 875.
- (29) Burrell, H. *Ind. Eng. Chem.* **1954**, *46*, 2233.

temperature of a two-layer coating with different thermal expansivity layers have been dealt with in detail in the literature.^{4–6,30–36} This paper therefore examines the wrinkling of the top layer when it generates in-plane compressive stress by absorbing solvents. It is further assumed that only the top layer wrinkles and the bottom layer conformed to the wrinkled shape upon wrinkling. The top layer is assumed to be a cross-linked elastic gel, and the bottom layer is assumed to be either elastic or viscous.

The remainder of the paper is divided into two sections. In the first section, a theory based on the Flory–Rehner rubber elasticity is presented to predict the value of in-plane compressive stress generated in a confined, elastic gel layer due to the absorption of solvent. The theory explains the effect of the concentration of elastically active cross-links (chemical or physical) and the affinity of the solvent for the gel on the equilibrium solvent content and the generated in-plane compressive stress. In the second section, stability analysis of such a swelled, compressed, elastic gel layer attached to either a viscous or an elastic bottom layer atop a rigid substrate is considered. This section identifies the critical conditions for wrinkling and predicts the wavelength and amplitude of the wrinkles formed. If the bottom layer is viscous, the compressed top layer is always unstable, and wrinkling is a kinetic process. The viscous flow of the bottom layer controls the kinetics, and selects the fastest growing wavelength.³⁷ If the bottom layer is elastic, there exists a critical compressive stress, beyond which the top layer wrinkles. The selected wrinkle wavelength is the one at which the total energy of the top and the bottom layer is minimized.³⁷ The goal of this paper is to examine the effects of the modulus of the top and bottom (when applicable) layer, the polymer solvent interaction parameter, and the thickness ratio of the bottom to top layer on the critical conditions of wrinkling, and the wrinkle wavelength and amplitude for the cases of viscous and elastic bottom layers.

2. Generation of Compressive Stress in a Confined Coating Layer by Solvent Absorption.

When exposed to a solvent, a *free* cross-linked gel layer swells to its equilibrium, stress-free state by absorbing solvent. Such a gel layer by virtue of being chemically cross-linked can absorb solvent only up to an equilibrium concentration. When the gel layer is *confined* to a rigid substrate, it can only swell freely in the direction perpendicular to the substrate, but not in the direction in-plane to the substrate. Therefore, swelling is frustrated in the in-plane direction. This frustrated in-plane swelling creates in-plane compressive stresses in the coating.³⁸

The in-plane compressive stress generated by frustrated swelling opposes solvent absorption and reduces the equilibrium solvent concentration in the cross-linked gel layer. The equilibrium solvent concentration depends on the swellability of the gel layer (which falls with rising concentration of cross-links) and the affinity of the solvent for the gel. The in-plane compressive stress depends on the modulus of the gel layer that is proportional

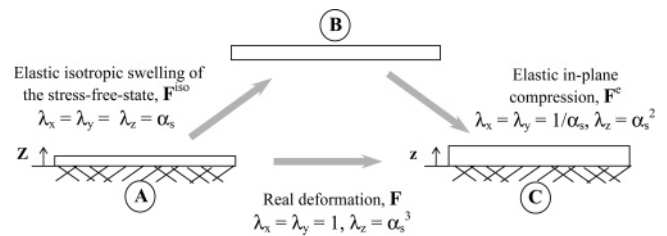


Figure 1. Schematic representation of the steps involved in the swelling of a confined gel layer. Here x and y are the in-plane coordinates, and z is the out-of-plane coordinate.

to the concentration of cross-links and the in-plane strain that depends on equilibrium solvent content. The modulus of the gel layer apart from being proportional to the concentration of cross-links also depends on equilibrium solvent concentration. To predict the equilibrium solvent concentration and the in-plane compressive stress generated, and to examine their dependence on the concentration of cross-links and the affinity of the solvent for the gel, a free-energy-based model of the swelling process is constructed.

Swelling of a confined gel layer is shown as a combination of two hypothetical steps in Figure 1. Linear strains in each coordinate direction (λ_x , λ_y , and λ_z) for each step are also indicated in the Figure. In the first step, the dry gel layer, which is attached to the substrate (state A) is detached and allowed to swell freely and isotropically to its equilibrium, completely relaxed, stress-free state (state B).⁴² In the second step, the stress-free, swelled layer is elastically compressed in-plane to its original in-plane dimension and reattached to the substrate (state C). Thus, the overall swelling process (state A to state C) is frustrated in the in-plane direction and this frustrated swelling generates in-plane compressive stress. The overall swelling process (A to C) can be represented by the deformation gradient tensor, \mathbf{F} .

$$\mathbf{F} \leftrightarrow \begin{bmatrix} 1 & 0 & 0 \\ 0 & 1 & 0 \\ 0 & 0 & \frac{\partial z}{\partial Z} \end{bmatrix} \quad (1)$$

where the lowercase z denotes the out-of-plane coordinate after swelling, and the uppercase Z denotes the same before swelling. As explained before, this overall deformation is composed of two steps: isotropic swelling to the stress-free state (\mathbf{F}^{iso}) followed by in-plane elastic compression to the original in-plane dimension (\mathbf{F}^{c}).

$$\mathbf{F} = \mathbf{F}^{\text{iso}} \cdot \mathbf{F}^{\text{c}} \quad (2)$$

The deformation gradient tensor for the isotropic swelling can be written as

$$\mathbf{F}^{\text{iso}} = \alpha_s \mathbf{I} \quad (3)$$

where α_s is the linear expansion ($\lambda_x = \lambda_y = \lambda_z = \alpha_s$) of the isotropically swelled gel. The determinant of \mathbf{F}^{iso} gives the ratio of the volume of gel after and before swelling. Further, if the gel is considered incompressible, this ratio is also related to the ratio of the gel volume fraction (ϕ_2) before and after swelling. In the remainder of this article, solvent is denoted by subscript

(30) Huck, W. T. S.; Bowden, N.; Onck, P.; Pardo, T.; Hutchinson, J. W.; Whitesides, G. M. *Langmuir* **2000**, *16*, 3497.

(31) Lacopi, F.; Brongersma, S. H.; Maex, K. *Appl. Phys. Lett.* **2003**, *82*, 1380.

(32) Yoo, P. J.; Suh, K. Y.; Park, S. Y.; Lee, H. H. *Adv. Mater.* **2002**, *14*, 1383.

(33) Yoo, P. J.; Park, S. Y.; Kwon, S. J.; Suh, K. Y.; Lee, H. H. *Appl. Phys. Lett.* **2003**, *83*, 4444.

(34) Kim, J.; Lee, H. H. *J. Polym. Sci., Part B: Polym. Phys.* **2001**, *39*, 1122.

(35) Zhang, H. L.; Okayasu, T.; Bucknall, D. G. *Eur. Polym. J.* **2004**, *40*, 981.

(36) Chua, D. B. H.; Ng, H. T.; Li, S. F. Y. *Appl. Phys. Lett.* **2000**, *76*, 721.

(37) Huang, R. *J. Mech. Phys. Solids* **2005**, *53*, 63.

(38) When a single gel layer is attached to a rigid substrate, high enough in-plane compressive stress can buckle it out of plane to produce wrinkles.³⁹ However, most often, such out-of-plane deformations cause delamination from the substrate and create blisters.^{40,41}

(39) Tanaka, T.; Sun, S. T.; Hirokawa, Y.; Katayama, S.; Kucera, J.; Hirose, Y.; Amiya, T. *Nature* **1987**, *325*, 796.

(40) Teschke, O.; Kleinke, M. U.; Galembeck, F. *J. Appl. Polym. Sci.* **1995**, *57*, 1567.

(41) Sharp, J. S.; Jones, R. A. L. *Adv. Mater.* **2002**, *14*, 799.

(42) Lei, H.; Francis, L. F.; Gerberich, W. W.; Scriven, L. E. *AIChE J.* **2002**, *48*, 437.

1, and gel is denoted by subscript 2. The dry gel layer in state A does not contain any solvent ($\phi_2^A = 1$), and, once swelled, the equilibrium polymer volume fraction does not change during the elastic in-plane compression step ($\phi_2^B = \phi_2^C = \phi_{2,e}$, where $\phi_{2,e}$ is the equilibrium gel volume fraction of the constrained gel layer).

$$\det \mathbf{F}^{\text{iso}} = \alpha_S^3 = \frac{V_B}{V_A} = \frac{\phi_2^A}{\phi_2^B} = \frac{1}{\phi_{2,e}} \quad (4)$$

The equilibrium solvent content in the gel layer can be predicted by using the fact that, at equilibrium, the chemical potential of the solvent inside and outside the gel is equal. The chemical potential of the solvent can be estimated from the Gibbs free energy (ΔG) of the confined gel–solvent system. The Gibbs free energy has two parts: one due to the mixing of solvent and polymer gel (ΔG_m), and the other due to the elastic deformation of the swelling gel (ΔG_{el}).⁴³

$$\Delta G = \Delta G_m + \Delta G_{el} \quad (5)$$

The former part can be estimated by the Flory–Huggins mixing free energy, with no contribution to the entropy of mixing from the immobile gel.⁴⁴

$$\Delta G_m = RT[n_1 \ln \phi_1 + \chi n_1 \phi_2] \quad (6)$$

where χ represents the interaction energies between the solvent and the cross-linked gel, and n_1 represents the number of moles of the solvent. The elastic part of the free energy is assumed to be purely entropic. It can be estimated from a modified rubber elasticity theory⁴⁴

$$\Delta G_{el} = \frac{-k\nu^e}{2} [\lambda_x^2 + \lambda_y^2 + \lambda_z^2 - 3 - \ln(\lambda_x \lambda_y \lambda_z)] \quad (7)$$

where ν^e is the number of elastically effective cross-links.

The difference in the chemical potential of the solvent inside the swollen network (μ_1) and that of the surrounding pure solvent (μ_1^0) is given by

$$\mu_1 - \mu_1^0 = \Delta\mu_1 = \left(\frac{\partial \Delta G}{\partial n_1} \right)_{T,p} \quad (8)$$

At equilibrium, the chemical potential of the solvent inside and outside the gel is equal. Equations 3–8 can be used to estimate the chemical potential difference of the solvent inside and outside of a *free* gel layer (state A to B) at equilibrium:

$$\Delta\mu_1 = RT \left[\ln(1 - \phi_{2,e}) + \phi_{2,e} + \chi \phi_{2,e}^2 + \frac{\nu^e \hat{V}_1}{V_A N_{av}} \left(\phi_{2,e}^{1/3} - \frac{\phi_{2,e}}{2} \right) \right] = 0 \quad (9)$$

where N_{av} is Avogadro's number, and \hat{V}_1 is the molar volume of the solvent. The factor ν^e/V_A is the moles of elastically effective cross-links per unit volume of original gel (state A). Arguments similar to those in eq 4 show that the determinant of the deformation gradient tensor \mathbf{F} of the original deformation (A to C) can be expressed as

$$\det \mathbf{F} = \frac{\partial z}{\partial Z} = \frac{V_C}{V_A} = \frac{\phi_2^A}{\phi_2^C} = \frac{1}{\phi_{2,e}} \quad (10)$$

Equations 5–8 and 10 can be used to estimate the chemical potential difference of the solvent inside and outside of a *confined* gel layer (state A to C) at equilibrium:

$$\Delta\mu_1 = RT \left[\ln(1 - \phi_{2,e}) + \phi_{2,e} + \chi \phi_{2,e}^2 + \frac{\nu^e \hat{V}_1}{V_A N_{av}} \left(\frac{1}{\phi_{2,e}} - \frac{\phi_{2,e}}{2} \right) \right] = 0 \quad (11)$$

Equation 11 can be solved numerically to estimate the equilibrium solvent concentration. This absorbed solvent in the attached gel layer generates in-plane compressive stress. The in-plane elastic compressive stress arises because of the in-plane elastic compression of the swelled gel, \mathbf{F}^e (state B to state C).

$$\mathbf{F}^e = \frac{1}{\alpha_S} \mathbf{F} \quad (12)$$

The determinant of \mathbf{F}^e is related to the gel volume ratio after and before deformation, and the swelled gel is considered incompressible:

$$\det \mathbf{F}^e = \frac{1}{\alpha_S^3} \frac{\partial z}{\partial Z} = \frac{V_C}{V_B} = 1 \quad (13)$$

The elastic stress tensor $\boldsymbol{\sigma}$ (of state C) can be calculated with the neo-Hookean constitutive equation. This constitutive equation can be derived from the rubber-elasticity free energy⁴⁵ eq 7:

$$\boldsymbol{\sigma}^e = -p\mathbf{I} + G^B \mathbf{B}^e \quad (14)$$

where $\mathbf{B}^e = \mathbf{F}^e \cdot \mathbf{F}^{eT}$ is the left Cauchy–Green tensor, and p is the unknown hydrostatic pressure, which can be predicted with the boundary condition $\sigma_{zz} = 0$ (no out of plane stress). The modulus of the swelled gel G^B (state B) is a function of the gel volume fraction at equilibrium $\phi_{2,e}$ and is linearly proportional⁴⁶ to the concentration of cross-links ν^e/V_A :

$$G^B = \frac{kT\nu^e \phi_{2,e}^{1/3}}{V_A} = G^A \phi_{2,e}^{1/3} \quad (15)$$

The factor $\phi_{2,e}^{1/3}$ appears because the gel in state B is isotropically swollen. With eqs 4 and 12–15 the in-plane stresses can be expressed as

$$\sigma_{xx} = \sigma_{yy} = kT \frac{\nu^e}{V_A} \left(\phi_{2,e} - \frac{1}{\phi_{2,e}} \right) \quad (16)$$

In-plane stress in the confined gel layer is a function of the concentration of cross-links and the equilibrium gel volume fraction. Since the modulus of the dry gel is proportional to the concentration of cross-links (eq 15), it is used as the parameter of choice in place of the concentration of cross-links in the remainder of the article. Also, water is considered the solvent in the remainder of the article, and its specific molar volume ($\hat{V}_1 = 18 \text{ cc/gmol}$) is used in all the predictions.

(43) Flory, P. J.; Rehner, J. *J. Chem. Phys.* **1943**, *11*, 512.

(44) Flory, P. J. *Principles of Polymer Chemistry*; Cornell University Press: Ithaca, NY, 1953.

(45) Basar, Y.; Weichert, D. *Nonlinear Continuum Mechanics of Solids*; Springer: Berlin, 2000.

(46) Hiemenz, P. C.; Lodge, T. P. *Polymer Chemistry*; University of Minnesota: Minneapolis, MN, 2004.

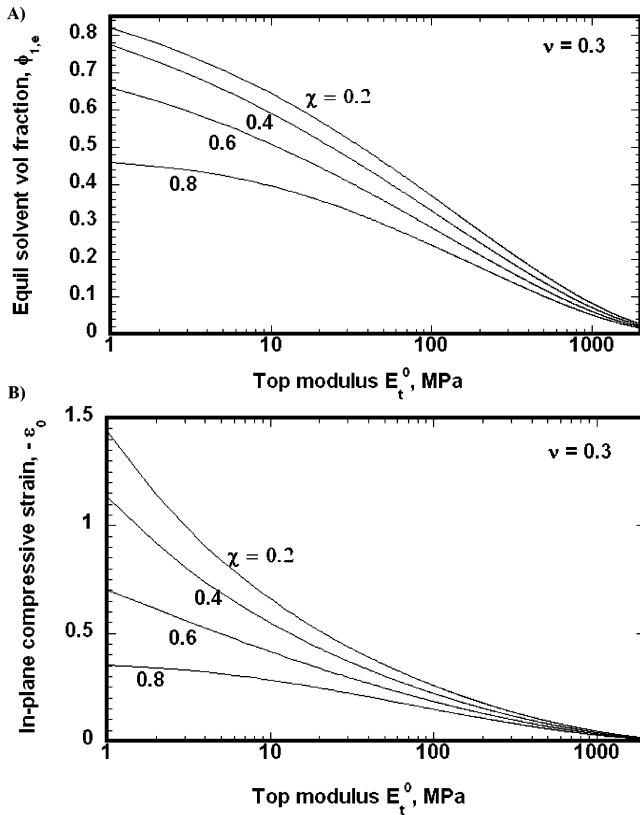


Figure 2. (A) Equilibrium solvent volume fraction and (B) in-plane compressive strain at equilibrium solvent content versus the Young's modulus of the gel layer for various values of χ .

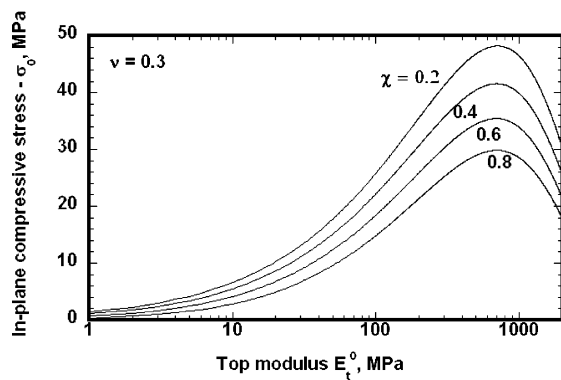


Figure 3. In-plane compressive stress at equilibrium solvent content versus Young's modulus of the gel layer for various values of χ .

Figure 2A plots the equilibrium solvent volume fraction in a confined gel layer (predicted from eq 11) versus Young's modulus of the unswollen gel layer (E_t^0) for various values of χ . The equilibrium solvent volume fraction falls as the modulus of the gel layer rises because the swellability of the gel falls with rising modulus. The equilibrium solvent volume fraction rises as χ falls because better solvents have higher affinity for the gel. The in-plane compressive strain, shown in Figure 2B, also falls as the equilibrium solvent volume fraction falls with rising modulus and χ . In-plane compressive stress, as shown in Figure 3, peaks with rising modulus and rises with falling χ . As the modulus rises, in-plane compressive strain falls, but the modulus rises causing the in-plane compressive stress, which is the product of the two, to peak. In-plane compressive stress rises with falling χ because better solvent raises the equilibrium solvent volume fraction and in-plane compressive strain.

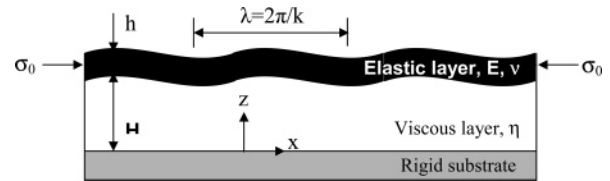


Figure 4. Schematic representation of the buckling of an elastic top layer bonded to a viscous bottom layer atop a rigid substrate under in-plane compression.

3. Wrinkling of the Top Layer of a Two-Layer Coating

This section utilizes key results from existing literature on the buckling analysis of a compressed elastic top layer atop a viscous or elastic bottom layer to investigate the wrinkling of a swelled, compressed, elastic gel layer bonded to a viscous or elastic bottom layer. The effects of the physical properties of the gel layer, namely, the modulus (degree of cross-linking), polymer solvent interaction parameter, and thickness ratio of the bottom to top layer on the critical conditions for buckling instability, wrinkle wavelength, and amplitude for both these cases are examined.

3.1. Wrinkling of an Elastic Gel Top Layer Bonded to a Viscous Bottom Layer. Several recent studies have examined the buckling instability of an elastic layer in compression bonded to a viscous underlayer.^{47–50} Sridhar et al.⁴⁹ performed a linear stability analysis of the elastic layer for small perturbations, but they neglected the shear traction at the layer interface and the in-plane displacements. Huang et al.⁴⁷ showed that such simplifications are incorrect when the thickness of the viscous layer is small. Huang et al.⁴⁸ also studied the buckling of the same system by approximating the viscous flow by lubrication theory and using nonlinear plate theory for the elastic film. Lubrication approximation required the thickness of the viscous layer to be small compared to the buckling wavelength, and therefore their analysis is not valid when the thickness of the viscous layer is large. Huang et al.⁴⁷ carried out a linear stability analysis of the same system using creeping flow in the viscous layer and using linear plate theory for the elastic film. Their analysis is valid for any thickness of the viscous layer and reduces to results from other authors in the thin⁴⁸ and thick⁴⁹ viscous layer limits.

A schematic representation of the buckling of an elastic layer of thickness h bonded to a viscous layer of thickness H , which in turn is bonded to a rigid substrate, is presented in Figure 4. The elastic layer is under in-plane biaxial compressive stress σ_0 . The biaxial compressive stress is related to the biaxial strain by $\sigma_0 = E_t \epsilon_0 / (1 - \nu)$, where E_t is the modulus and ν is the Poisson's ratio of the elastic layer. When the elastic top layer is a cross-linked gel, its modulus $E_t = E_t^0 \phi_{2,e}^{1/3}$ is a function of the equilibrium gel volume fraction $\phi_{2,e}$. The governing equations and major results of the linear stability analysis of the elastic layer are presented by Huang et al.⁴⁷ According to their analysis, for a given value of the compressive strain, the elastic layer is unstable to perturbations of higher wavelength than a critical wavelength λ_c :

$$\frac{\lambda_c}{h} = \frac{2\pi}{\sqrt{-12\epsilon_0(1 + \nu)}} \quad (17)$$

The critical wavelength λ_c is nonimaginary only when the in-

(47) Huang, R.; Suo, Z. *Int. J. Solids Struct.* **2002**, *39*, 1791.

(48) Huang, R.; Suo, Z. *J. Appl. Phys.* **2002**, *91*, 1135.

(49) Sridhar, N.; Srolovitz, D. J.; Suo, Z. *Appl. Phys. Lett.* **2001**, *78*, 2482.

(50) Sridhar, N.; Srolovitz, D. J.; Cox, B. N. *Acta Mater.* **2002**, *50*, 2547.

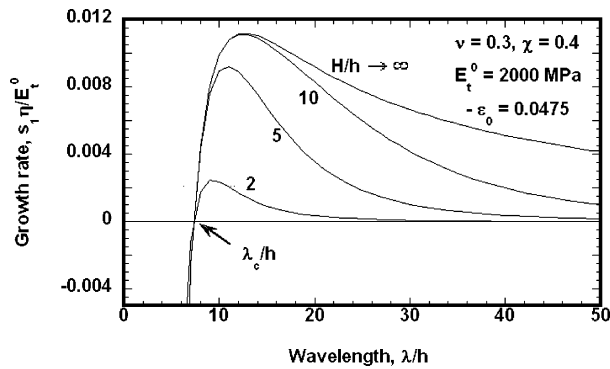


Figure 5. Growth rate of the linear perturbation versus wavelength for various thickness ratios of a top layer with a Young's modulus of 2000 MPa. At equilibrium solvent content, such a layer would experience an in-plane compressive strain, $-\epsilon_0 = 0.0475$.

plane strain is compressive ($\epsilon_0 < 0$). When the in-plane strain is tensile ($\epsilon_0 > 0$) or the layer is strain-free ($\epsilon_0 = 0$), then perturbation decays and the layer is stable. When the in-plane strain (or stress) is compressive, the critical wavelength is the result of compromise between energy reduction associated with the expansion of the layer and energy addition associated with bending out of plane. For a given value of in-plane compressive stress, when $\lambda < \lambda_c$, the growth rate is negative, perturbation decays, and the planar state is stable. When $\lambda > \lambda_c$, the growth rate is positive, therefore perturbation grows exponentially, and the planar state is unstable. Large (small) wavelength perturbations grow (decay) since the energy reduction associated with expansion of the layer is more (less) than the energy addition associated with bending out of plane. This is shown graphically in Figure 5, where the dimensionless growth rate of perturbations (predicted from eqs 11–13, 29–30, and 33–34 of Huang et al.⁴⁷) in a cross-linked elastic gel layer that has absorbed an equilibrium amount of solvent is plotted against the wavelength for different ratios of bottom layer to top layer thickness. The critical wavelength for wrinkling is the same as that for a free-standing layer subjected to in-plane compression. The viscous bottom layer cannot exert any traction on the elastic top layer unless it begins to flow. Therefore, the viscosity of the viscous layer or its thickness does not have any effect on the critical condition for instability. However, the viscosity and thickness of the bottom layer determine the growth rate of unstable modes. Figure 5 shows that, for a given thickness ratio, the growth rate peaks as wavelength rises. Shorter wavelength wrinkles decay because the bending energy is too high compared to the energy of expansion, and higher wavelength wrinkles grow slowly because it takes a long time for the viscous material below to flow to accommodate the long wavelength wrinkles; hence, the wrinkles with intermediate wavelength grow fastest.

The evaluation of perturbation amplitude presented by Huang et al.⁴⁷ (eqs 31–32) is valid for small times only: once the perturbation amplitude becomes large compared with the elastic layer thickness, linear stability analysis no longer provides an accurate description of the film profile evolution. In the long time limit, for a fixed wavelength, there would be a thermodynamic, equilibrium amplitude corresponding to a balance between the release of the compressive stress in the layer and the energy of bending the layer out of plane. Huang et al.⁴⁸ found the equilibrium amplitude for any perturbation wavelength λ as a function of critical wavelength λ_c .

$$\frac{A}{h} = \left(\frac{1}{3} \left[\left(\frac{\lambda}{\lambda_c} \right)^2 - 1 \right] \right)^{1/2} \quad (18)$$

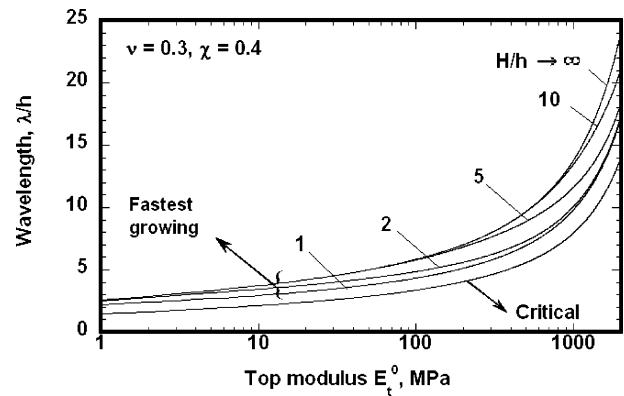


Figure 6. Fastest growing and critical wavelengths versus Young's modulus of the top layer for various thickness ratios. The critical wavelength does not depend on thickness ratios.

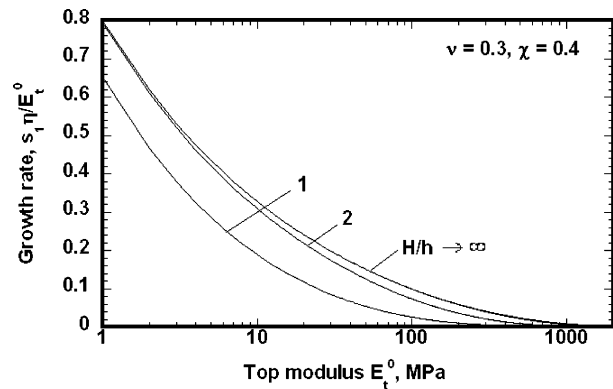


Figure 7. Growth rate of the fastest growing wavelengths versus Young's modulus of the top layer for various thickness ratios.

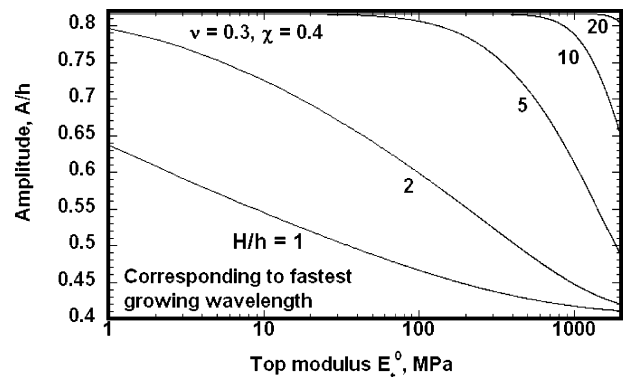


Figure 8. Equilibrium amplitudes of the fastest growing wavelengths versus Young's modulus of the top layer for various thickness ratios.

For $\lambda < \lambda_c$, the equilibrium amplitude is nonexistent, and the flat top layer is stable.

The wrinkle wavelength most likely to be observed at equilibrium is the one growing fastest. The fastest growing wavelength λ_m , obtained from $\partial(\text{growth rate})/\partial\lambda = 0$, is plotted in Figure 6, along with the critical wavelength λ_c , against the modulus of the top layer for various bottom to top layer thickness ratios H/h . As shown earlier in Figure 5, the critical wavelength λ_c is independent of H/h . Growth rates and equilibrium amplitudes of the fastest growing perturbations for various H/h ratios are plotted in Figures 7 and 8, respectively. The fastest growing wavelength rises and the equilibrium amplitude falls because the bending stiffness of the elastic layer rises with its modulus. The growth rate of the perturbations falls with rising elastic layer modulus. Therefore, coatings with high elastic gel layer moduli

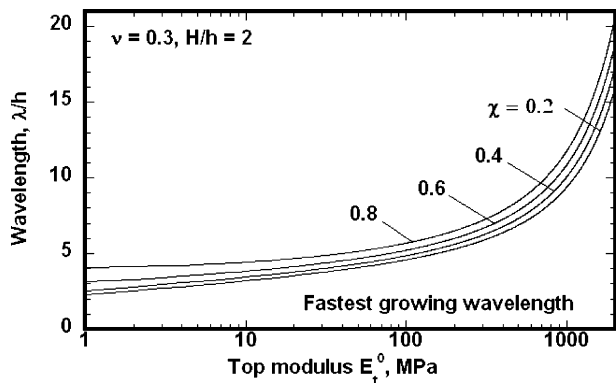


Figure 9. Effect of χ on the fastest growing wavelength. The result for a representative value of $H/h (= 2)$ is shown.

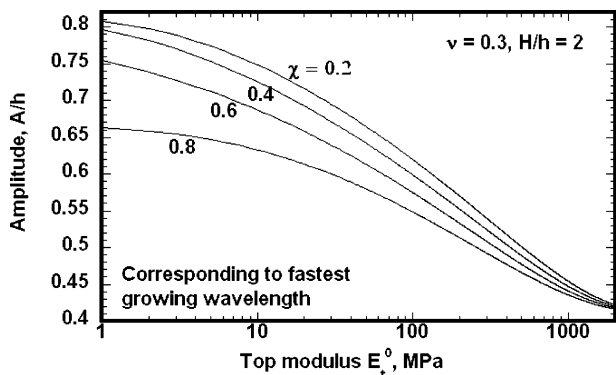


Figure 10. Effect of χ on the amplitude corresponding to the fastest growing wavelength. The result for a representative value of $H/h (= 2)$ is shown.

generate high-wavelength, low-amplitude wrinkles that grow slowly; simply put, such coatings are least likely to wrinkle.

The fastest growing wavelength and the equilibrium amplitude rise as H/h rises because the constraint of the rigid substrate to the out-of-plane deformation of the elastic gel layer diminishes with rising H/h . However, as the viscous layer becomes infinitely thick, both the fastest growing wavelength and the equilibrium amplitude saturate. The growth rate of the fastest growing wavelengths also rises with rising H/h because the constraint of the rigid substrate to the flow in the viscous layer diminishes with rising H/h .

The fastest growing wavelengths and the corresponding equilibrium amplitudes are plotted against the modulus of the top layer for various values of the polymer solvent interaction parameter χ in Figures 9 and 10, respectively. The fastest growing wavelength falls, and the equilibrium amplitude rises as the affinity of the solvent for the gel rises (χ falls) because better solvents create higher compressive strain that promotes low-wavelength, high-amplitude wrinkles.

3.2. Wrinkling of an Elastic Gel Top Layer Bonded to an Elastic Bottom Layer. The buckling of a compressed elastic layer bonded to another elastic layer has been analyzed by many authors.^{16,24,25,28,37,51–54} Allen²⁴ analyzed the buckling problem by approximating the deformation of the top layer by Euler’s linear plate theory, and the linear elasticity with the Hookean constitutive equation for the bottom layer. However, he did not consider the shear stress at the interface of the layers and neglected the in-plane displacements. Groenewold⁵² analyzed the same

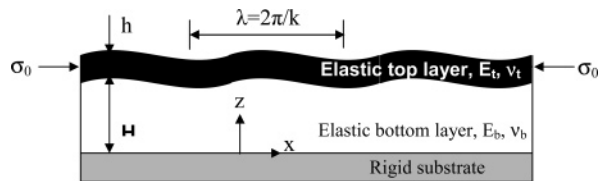


Figure 11. Schematic representation of the buckling of an elastic top layer bonded to an elastic bottom layer atop a rigid substrate under in-plane compression.

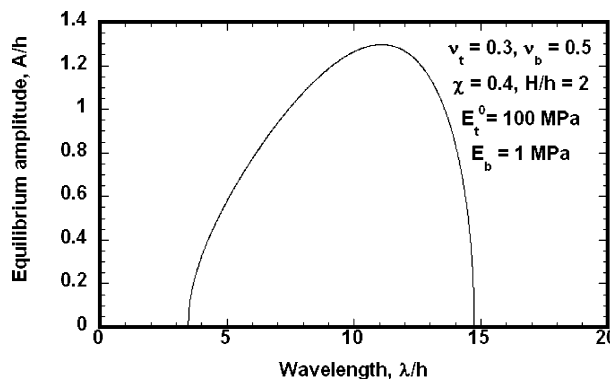


Figure 12. Equilibrium wrinkle amplitude versus wrinkle wavelength.

buckling problem by minimizing the bending and the compressive energy of both the layers together with slightly different boundary conditions than Allen, but obtained similar results.

A schematic representation of the buckling of an elastic top layer of thickness h bonded to another elastic bottom layer of thickness H , which in turn is bonded to a rigid substrate, is presented in Figure 11. The top layer is biaxially compressed by compressive stress σ_0 . The top and the bottom layers have moduli E_t and E_b and Poisson’s ratios ν_t and ν_b , respectively. Huang³⁷ analyzed the buckling of the top layer by modeling the deformation of the top layer by von Karman’s nonlinear plate theory. The nonlinearity of von Karman’s plate theory allowed him to obtain the equilibrium amplitude of the wrinkles as a function of the in-plane compressive stress, wavenumber, E_b/E_t , and H/h (equation 3.2 of Huang et al.³⁷):

$$A = \frac{\lambda \sqrt{1 - \nu_t^2}}{\pi} \left[-\frac{\sigma_0}{E_t} - \frac{\pi^2 h^2}{3\lambda^2(1 - \nu_t^2)} - \frac{E_b \lambda}{\pi \gamma E_t h} \right]^{1/2} \quad (19)$$

where λ is the wavelength of the wrinkles, and γ is a function of the thickness and Poisson’s ratio of the bottom layer and the wavenumber (equation A.14 of Huang et al.³⁷):

$$\gamma = \frac{(1 - \nu_b)[(3 - 4\nu_b) \sinh(2kH) - 2kH]}{(3 - 4\nu_b) \cosh^2(kH) + (kH)^2 + (2\nu_b - 1)^2} \quad (20)$$

Here, $k = 2\pi/\lambda$ is the wavenumber of the wrinkles.

When the top layer is a cross-linked elastic gel that has absorbed an equilibrium amount of solvent, its modulus $E_t = E_t^0 \phi_{2,e}^{1/3}$ is a function of the equilibrium gel volume fraction $\phi_{2,e}$. The in-plane stress generated, σ_0 , is also a function of the equilibrium gel volume fraction and the concentration of elastically effective cross-links, and can be predicted from equations 11 and 16. Figure 12 shows the equilibrium wrinkle amplitude of a gel top layer that has absorbed an equilibrium amount solvent as a function of the wrinkle wavelength. Nonzero equilibrium amplitude exists only for an intermediate wavelength window. Outside the window equilibrium amplitude is zero, that is, the

(51) Chen, X.; Hutchinson, J. W. *J. Appl. Mech.* **2004**, *71*, 597.
 (52) Groenewold, J. *Physica A* **2001**, *298*, 32.
 (53) Chen, X.; Hutchinson, J. W. *Scr. Mater.* **2004**, *50*, 797.
 (54) Huang, Z.; Hong, W.; Suo, Z. *Phys. Rev. E.* **2004**, *70*, 030601.

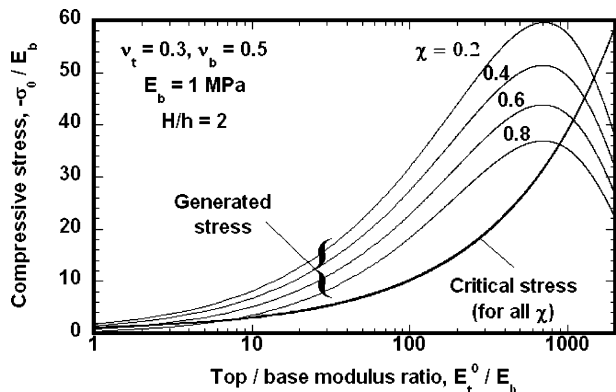


Figure 13. Critical compressive stress for wrinkling and compressive stress generated in the top layer at equilibrium solvent content versus the ratio of top to bottom layer Young’s moduli for various values of χ .

top layer does not wrinkle. The bending stiffness of the top layer disfavors the low-wavelength wrinkles, and the constraint of the bottom layer disfavors the high-wavelength wrinkles, allowing the top layer to wrinkle only at some intermediate wavelength window. It will be shown later that the window shrinks as the top and bottom layer moduli and/or χ rise, and/or the thickness ratio H/h falls. Therefore, a critical condition exists where the equilibrium amplitude is zero at all wavelengths and the flat top layer is stable. The critical compressive stress can be predicted by treating σ_0 as an unknown and setting the maximum equilibrium amplitude of eq 19 to zero.

Figure 13 shows the critical compressive stress as a function of the top layer modulus E_t for various values of χ and given values of E_b and H/h . The critical compressive stress is a weak function of χ : plots for various values of χ fall on top of each other. The plot for the critical compressive stress divides the plane into two regions: below the plot the top layer is stable, and, above the plot, the top layer wrinkles. For a given top layer modulus, the critical condition predicts the minimum compressive stress required to wrinkle the top layer. For a given compressive stress, the critical condition predicts the maximum value of E_t for the top layer to wrinkle. The critical compressive stress of the top layer rises with E_t because the bending stiffness of the top layer rises with E_t .

Figure 13 also plots the compressive stresses generated in the top layer that has absorbed an equilibrium amount of solvent for various values of χ and given values of E_b and H/h . The top layer will wrinkle only when the compressive stress generated is greater than the critical stress for wrinkling. For every value of χ , there exists a range of values of E_t for which the top layer would generate enough compressive stress to wrinkle. Figure 14 shows plots of wrinkling windows with E_t and χ as axes and E_b as the parameter. For a given value of E_b , the region below the curve shows combinations of E_t and χ that would produce wrinkles, and the region above the curve shows combinations that would not. As the value of χ rises, the equilibrium solvent content falls, causing the generated stress to fall below the critical stress for wrinkling. Further, the generated compressive stress peaks with rising values of E_t , causing the coatings with an intermediate top layer modulus and low χ to be the most prone to wrinkling. As E_b rises, the wrinkling window shrinks because the constraint of the bottom layer opposes the wrinkling of the top layer.

Figure 15 shows the critical compressive stress and the compressive stresses generated in the top layer that have absorbed an equilibrium amount of solvent as a function of the top layer modulus E_t for various values of H/h and given values of E_b and χ . For a given value of E_t , the critical stress for wrinkling falls

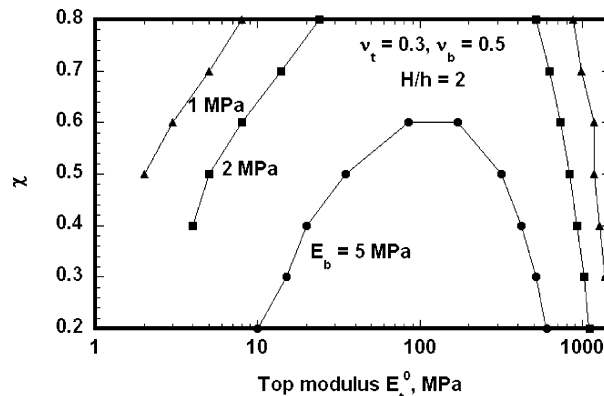


Figure 14. Wrinkling window with the top layer Young’s modulus and χ as axes and the bottom layer modulus as a parameter. For a given bottom layer modulus, any combination of top layer modulus and χ that falls below the corresponding line would produce wrinkles.

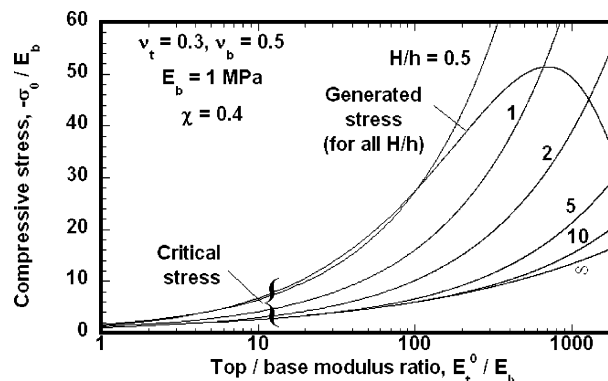


Figure 15. Critical compressive stress for wrinkling and compressive stress generated in the top layer at equilibrium solvent content versus the ratio of top to bottom layer Young’s moduli for various values of thickness ratio H/h .

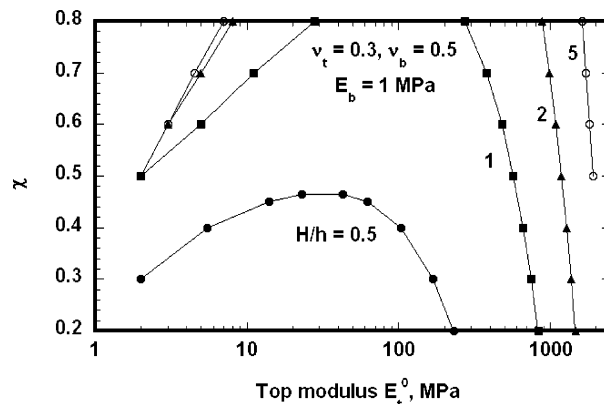


Figure 16. Wrinkling window with the top layer Young’s modulus and χ as axes and the thickness ratio H/h as a parameter. For a given value of H/h , any combination of the top layer modulus and χ that falls below the corresponding line would produce wrinkles, and the region above the curve shows combinations that would not. As

as H/h increases because thicker bottom layers provide less constraint on wrinkling. However, the critical compressive stress becomes insensitive to the values of H/h as $H/h \rightarrow \infty$ because the presence of the rigid substrate no longer constrains wrinkling. The compressive stress generated depends solely on the concentration of elastically effective cross-links and χ and therefore does not change with H/h . Figure 16 shows plots of wrinkling windows with E_t and χ as axes and H/h as the parameter. For a given value of H/h , the region below the curve shows combinations of E_t and χ that would produce wrinkles, and the region above the curve shows combinations that would not. As

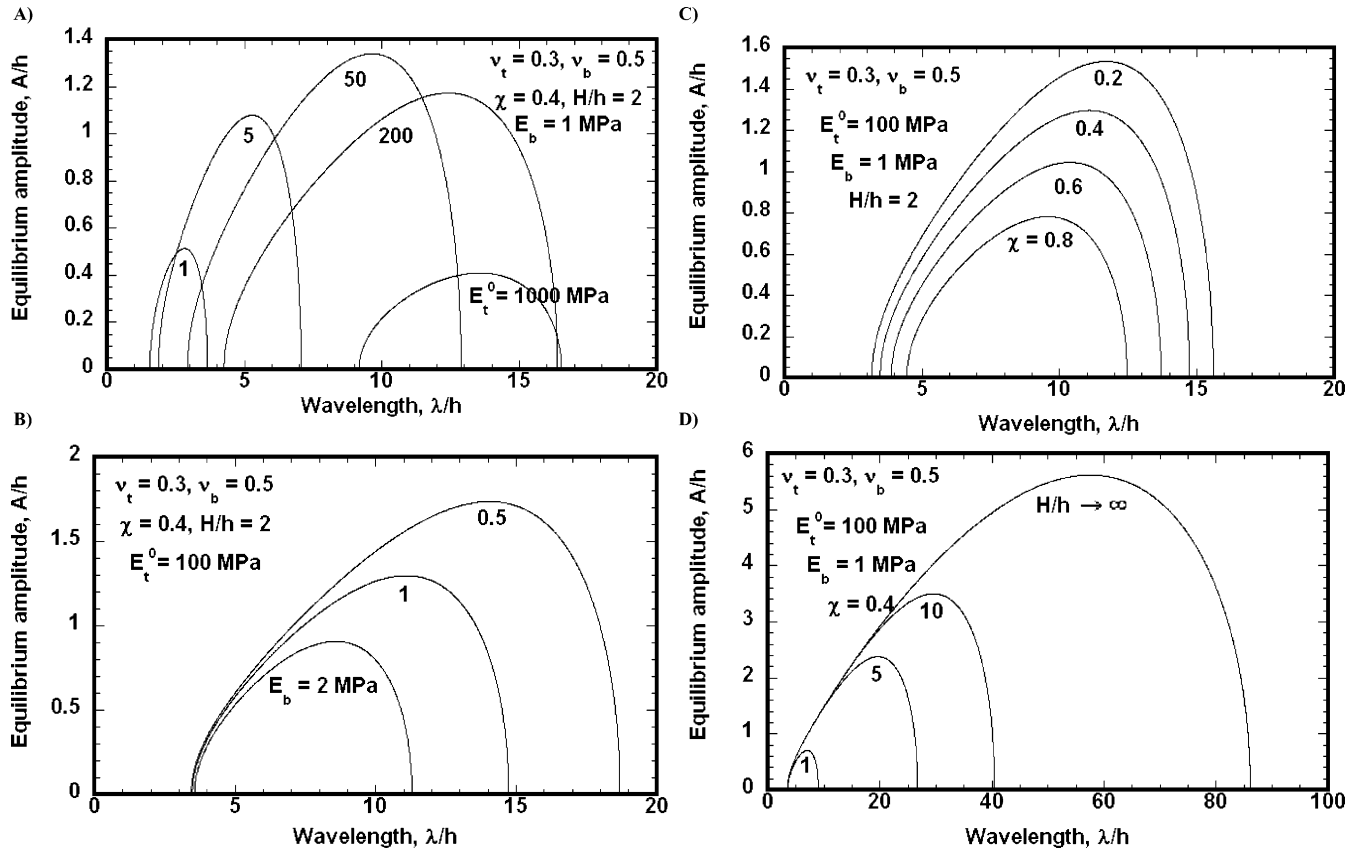


Figure 17. Equilibrium wrinkle amplitude versus wrinkle wavelength for various values of (A) the top layer modulus, (B) the bottom layer modulus, (C) χ , and (D) the thickness ratio H/h .

H/h falls, the wrinkling window shrinks because the proximity of the rigid substrate opposes the wrinkling of the top layer.

The maximum equilibrium amplitude peaks and the corresponding wavelength rises with the top layer modulus. Figure 17A shows the equilibrium amplitude of a gel top layer that has absorbed an equilibrium amount of solvent as a function of wrinkle wavelength for various values of top layer modulus and given values of E_b , H/h , and χ . The equilibrium solvent content, in-plane compressive strain, and therefore the stored compressive elastic strain energy that promotes wrinkling fall with rising top layer modulus. However, E_t/E_b rises, and therefore the constraint of the bottom layer that opposes wrinkling falls with rising top layer modulus. The interplay of these two opposing factors causes the equilibrium amplitude to peak. The wavelength rises with E_t because the bending stiffness of the top layer rises with E_t .

The maximum equilibrium amplitude and the corresponding wavelength fall with rising bottom layer modulus and given values of E_t , H/h and χ (Figure 17B). As E_b rises, the bottom layer disfavors out-of-plane deformation, and equilibrium amplitude falls. Also, as E_b rises, the constraint of the bottom layer rises, which disfavors long wavelength wrinkles.

The maximum equilibrium amplitude falls and the corresponding wavelength falls insignificantly with the falling affinity of the solvent for the gel (higher χ) and given values of E_t , E_b , and H/h (Figure 17C). As the affinity of the solvent for the gel falls, the equilibrium solvent content, in-plane compressive strain, and therefore the stored compressive elastic strain energy that drives wrinkling fall, causing the equilibrium amplitude to fall.

The maximum equilibrium amplitude and the corresponding wavelength rise with the rising bottom layer to top layer thickness ratio H/h and given values of E_t , E_b , and χ (Figure 17D). As H/h rises, the constraint of the bottom layer that disfavors wrinkling falls, causing the wrinkle amplitude and wavelength to rise.

However, the effect of H/h on wrinkle amplitude and wavelength diminishes as $H/h \rightarrow \infty$ because the presence of the rigid substrate no longer constrains wrinkling.

4. Conclusions

An in-plane constrained cross-linked gel layer absorbs an equilibrium amount of solvent and experiences in-plane compressive stress. The equilibrium solvent content can be predicted by setting the chemical potential difference of the solvent inside and outside the gel equal to zero. The equilibrium solvent content is a function of the concentration of cross-links and the polymer solvent interaction parameter χ . The in-plane compressive stress can be predicted from a rubber elasticity constitutive equation and is also a function of the concentration of cross-links and the polymer solvent interaction parameter χ . The equilibrium solvent content and in-plane compressive strain fall with rising concentration of cross-links and falling affinity of the solvent for the gel. However, the in-plane compressive stress peaks with rising concentration of cross-links because swellability and in-plane compressive strain fall and modulus rise with rising concentration of cross-links. The in-plane compressive stress falls with falling affinity of the solvent for the gel.

Stability analysis of a cross-linked elastic gel that has absorbed an equilibrium amount of solvent and attached to either a viscous or elastic bottom layer can be used to examine the effect of the top and bottom layer modulus, the thickness ratio of the layers, and the polymer solvent interaction parameter on the critical conditions of wrinkling, and the wrinkle wavelength and amplitude. When the bottom layer is viscous, the compressed top layer is always unstable, and wrinkling is a kinetic process. The viscous flow of the bottom layer controls the kinetics and selects the fastest growing wavelength that is most likely to be

observed at equilibrium. As the elastic gel layer modulus rises, the fastest growing wavelength rises and the equilibrium amplitude falls because the bending stiffness of the elastic layer rises with its modulus. As the thickness ratio H/h rises, the fastest growing wavelength and the equilibrium amplitude rise because the constraint of the rigid substrate to the out-of-plane deformation of the elastic gel layer diminishes with rising H/h . As χ falls, the fastest growing wavelength falls and the equilibrium amplitude rises because better solvents create higher compressive strain that promotes low-wavelength, high-amplitude wrinkles.

When the bottom layer is elastic, there exists a critical compressive stress. If the generated compressive stress is greater than the critical stress, the top layer wrinkles. As the top layer modulus rises, the critical compressive stress rises, and the compressive stress generated peaks at an intermediate value, causing coatings with top layers of intermediate modulus to most likely wrinkle. Wrinkle amplitude peaks because the generated stress peaks, and wrinkle wavelength rises because bending stiffness rises with rising top layer modulus. As the bottom layer modulus rises, the critical compressive stress rises, but the

compressive stress generated does not change, so that coatings with a low bottom layer modulus are most likely to wrinkle. Wrinkle amplitude and wavelength fall because the constraint of the bottom layer rises with rising bottom layer modulus. As the thickness ratio H/h rises, the critical compressive stress falls, but the compressive stress generated does not change, so that coatings with high H/h are most likely to wrinkle. Wrinkle amplitude and wavelength rise because the proximity to the rigid substrate that opposes wrinkling falls with rising H/h . As χ falls, the critical compressive stress does not change, but the compressive stress generated rises; thus, coatings absorbing solvents with low χ are most likely to wrinkle. Wrinkle amplitude rises because better solvent generates higher compressive strain energy, which promotes wrinkling, and wavelength does not change significantly with falling χ .

Acknowledgment. This research was supported by the Industrial Partnership for Research in Interfacial and Materials Engineering (IPRIME, www.iprime.umn.edu).

LA060551O